

Precision Transducers Using Mechanical Resonators

Kinji Harada*, Kyoichi Ikeda**, Toshitsugu Ueda***, Fusao Kohsaka***, and Katsumi Isozaki***

We have long focused on the outstanding characteristics of mechanical resonators and directed intensive research toward finding applications. This paper describes mainly the structure, principles, and characteristics of a double-ended tuning fork resonator which combines two tuning forks, cylindrical resonator which consists of a thin-walled cylinder fixed at both ends, and transducers using these mechanical resonators for pressure, force, and density measurement.

Key Words: Mechanical Resonator, Double-ended tuning fork resonator, Cylindrical resonator

1. Introduction

It is well known from our daily experience that when tension is applied to a string or water is poured into a glass, its resonance frequency changes. Although attempts to use such elastic vibration, for a physical quality measurement have already been reported^{1) to 9)} and some have even been commercialized, their use has not yet become widespread.

While conventional transducers using mechanical resonators can offer very good repeatability, resolution, and stability, there is a nonlinear relationship between their inputs and outputs which requires complicated signal processing circuits. They also tend to have sensitive characteristics against external vibration. However, as digital signal processing has become much easier thanks to the remarkable progress in electronic technology, these frequency-output sensors have been greatly improved.

We have long focused on the outstanding characteristics of mechanical resonators and directed intensive research toward finding applications for advanced transducers by overcoming the conventional drawbacks with new technology.¹⁰⁾ This paper describes mainly the structure, principles, and characteristics of a double-ended tuning fork resonator which combines two tuning forks, cylindrical resonator which consists of a thin-walled cylinder fixed at both ends, and transducers using these mechanical resonators for pressure, force, and density measurement.

2. Double-ended Tuning Fork Resonator and Its Applications

The natural frequency f of an elastic beam is determined from only its material and structure, and is given by relationship (1):

$$f \propto \frac{1}{L} \left(\frac{E}{\rho} \right)^{1/2} \quad (1)$$

where

L : length of the beams (typical)

E : Young's modulus of beam material

ρ : density of the beam.

Thus if a resonator is designed so that its natural frequency varies with such a specific physical quantity as strain, force, pressure, or temperature, it can be used as transducers. The dual-ended tuning fork resonator is a transducer whose natural frequency varies with axial force (axial strain).

2.1 Structure and Principles of the Resonator^{11),12)}

As the natural frequency of the resonator varies with the amount of axial force applied to the beam, it can be a measure of the axial force. For a conventional single beam, however, it is difficult to obtain a resonator with a stable natural frequency. Because, the vibrational energy transmitting from the bearing to the outside changes due to the bearing conditions, leading to a low mechanical Q (a reciprocal of the mechanical damping factor).

We have devised a double-ended tuning fork

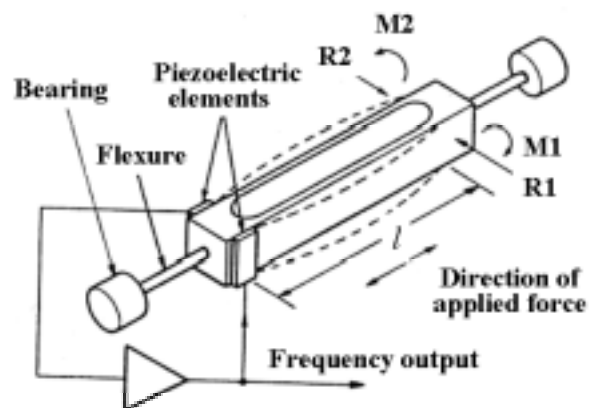


Figure 1. Structure of Dual-ended Tuning Fork Resonator

* Yokogawa Research Institute Corporation
2-9-32, Naka-cho, Musashino-shi, Tokyo 180-8750, Japan

** Department of Mechanical Systems Engineering
Tokyo University of Agriculture and Technology

*** Yokogawa Electric Corporation
2-9-32, Naka-cho, Musashino-shi, Tokyo 180-8750, Japan

resonator that overcomes such drawbacks. Figure 1 shows its structure. As the two beams vibrate symmetrically, vibrational counter forces R_1 and R_2 , and bending moments M_1 and M_2 cancel each other out, which eliminates any force applied to the bearing. As a result, the vibrational energy is trapped inside the resonator and its mechanical Q is high (1×10^4 or more). In addition, the flexure mountings at both ends of the resonator also reduce the effect of mounting status and external vibration. The natural frequency of the resonator can be measured by configuring a self-excitation oscillator circuit, which includes a pair of piezoelectric elements attached to nodes of vibrating beams for excitation and detection.

If the natural frequency of the resonator is f_0 when compressing axial force F is 0, the possible frequencies f of symmetrical vibration modes when a force is applied are given by equation (2).^{13), 14)}

$$f = f_0 \left\{ 1 - \frac{1}{a^3} \tanh \frac{a}{2} \left(a \tanh \frac{a}{2} - 2 \right) \frac{l^2 F}{2EI} \right\}^{1/2}$$

$$f_0 = \frac{a^2}{2\pi l^2} \left(\frac{EI}{\rho A} \right)^{1/2} \quad (2)$$

where

- a : value determined by mode number n of vibration
 $[\cong (1 + 2n)\pi/2]$
- E : Young's modulus of beam material
- I : resonator's second moment of inertia of area
- A : cross-section area of the resonator beam
- l : length of the beams
- ρ : density of the beam.

Thus the resonant frequency f is a measure of the applied axial force F .

2.2 Characteristics of the Resonator

Figure 2 shows an example of measured values of the frequency sensitivity ($\Delta f/f_0$) when applying a compressing axial force to the double-ended tuning fork resonator (effective length: 10 mm; thickness: 0.1 mm; width: 2 mm) shown in figure 1 for different vibration

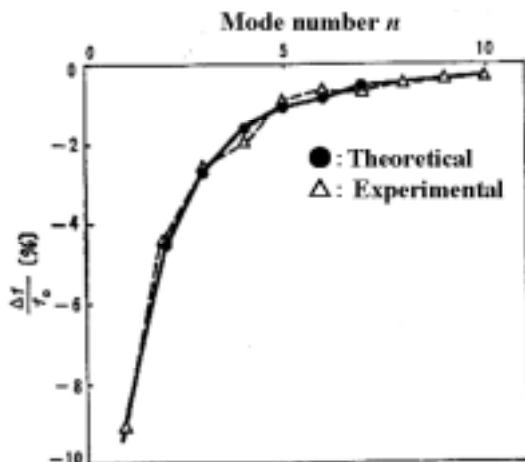


Figure 2. Relationship between Vibration Mode Numbers and Force (6 N) Sensitivity

mode numbers n . The measured values match the values calculated from equation (2).

If ε is the axial strain produced by applying an axial force F , substituting $F = 2\varepsilon EA$ in equation (2) gives:

$$f = f_0 \left\{ 1 - \frac{1}{a^3} \tanh \frac{a}{2} \left(a \tanh \frac{a}{2} - 2 \right) \frac{Al^2}{I} \varepsilon \right\}^{1/2} \quad (3)$$

Then the frequency sensitivity S_f , the frequency sensitivity per unit strain in the vicinity of f_0 , is given by:

$$S_f = \frac{1}{f_0} \frac{\partial f}{\partial \varepsilon} \cong -\frac{1}{a^3} \tanh \frac{a}{2} \left(a \tanh \frac{a}{2} - 2 \right) \frac{Al^2}{2I} \quad (4)$$

The value S_f for the first vibration mode ($n = 1$) is 1200 or more and is much larger than that for a wire resistance strain gauge or semiconductor strain gauge. This means that the resonator can operate even for small strains and increase repeatability and hysteresis characteristics, which is a major feature for resonator-type transducers.

Figure 3 shows the long-term stability of f_0 of a resonator made of a nickel alloy with a constant modulus of elasticity. Such a resonator with adequate stability can be manufactured by precisely controlling the temperature of heat treatment and the bonding method of piezoelectric elements.

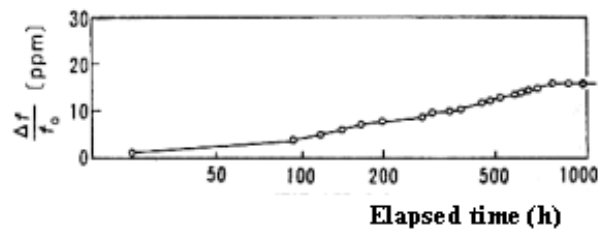


Figure 3. Aging Characteristics of Dual-ended Tuning Fork Resonator

2.3 Application to Pressure Transducer^{14),15)}

We have developed accurate pressure transducers using a dual-ended tuning fork resonator for

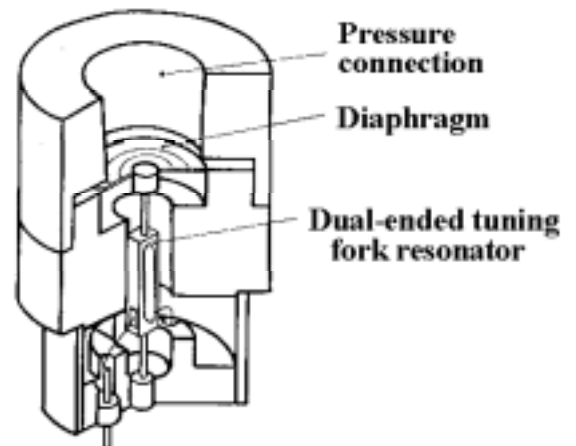


Figure 4. Structure of Pressure Transducer

three measuring ranges (0 to 20, 0 to 200, and 0 to 2000 kPa). All three transducers use the first vibration mode, which is highly sensitive, to achieve 10% of the rate of frequency change within the measuring range.

Figure 4 shows the structure of a pressure transducer. The upper end of the resonator is welded directly to the diaphragm and the lower end to the transducer body. It is a simple structure with fewer components. Moreover, the resonator does not come into contact with the measured fluid and thus is not affected by it. When the pressure to be measured is applied to the upper side of the diaphragm, the compressing axial force acts upon the resonator. Hence, this pressure transducer can measure gauge pressure if the chamber under the diaphragm is open to the atmosphere, and the absolute pressure if it is under vacuum. Three different diaphragms are designed for three measuring ranges. We have reduced the spring constant of the diaphragm to a tenth or less than that of the resonator, in consideration of a predominance of the resonator's superior characteristics.

The measured frequency is linearized according to the scale for each resonator, converted into an engineering unit, and zero adjusted by a microcomputer. In addition, if accurate measurement is required over a wide range of temperature, the pressure transducer can have an internal temperature transducer. It can be used to apply pulse amplitude modulation to the frequency cycle of a pressure signal with the temperature signal, and transfer both signals simultaneously to a microcomputer for compensation.

Actually, the frequency f is converted into the pressure P using the following equation (5), which is a modification of equation (2):

$$P = \sum_{n=1}^3 A_n \left(1 - \frac{f}{f_0} \right)^n \quad (5)$$

where

- f_0 : resonator frequency when $P = 0$
- A_n : constant.

Typical examples are given in figure 5, which shows the calibration characteristics of a pressure transducer with a measuring range of 0 to 200 kPa, and in figure 6, which shows the temperature characteristics before compensation. As aforementioned, compensating temperature with the internal transducer can further improve the accuracy of a pressure transducer to $\pm 0.01\%$ of the full scale when within 0°C to 50°C .



Figure 5. Calibration Characteristics of Pressure Transducer

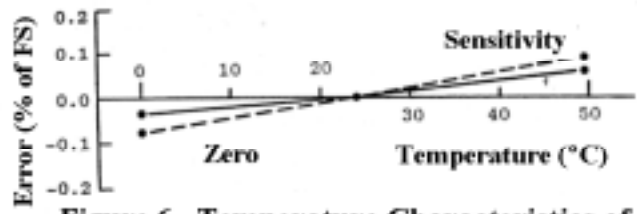


Figure 6. Temperature Characteristics of Pressure Transducer

2.4 Application to Electronic Balance¹⁶⁾

Figure 7 shows the basic structure of a single-pan electronic balance using the dual-ended tuning fork resonator as a force transducer. By adding weights to the pan, axial force is applied to the resonator through a Roberval's mechanism and lever. A single resonator can replace the small-displacement pickup mechanism and moving-coil force motor of electromagnetic balances, which are now in widespread use. The use of a resonator enables a simple structure to provide frequency output.

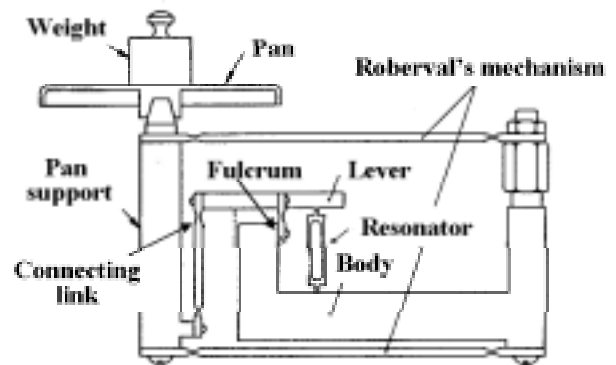


Figure 7. Structure of Electronic Balance

For two prototype electronic balances with weighing capacities of 200 g and 2 kg, the errors were 1 part in 10^5 of span for the 200-g balance and 1 part in 5×10^4 for the 2-kg balance. The structure of the circuit for converting frequency into mass is basically the same as the pressure transducer. However, as the electronic balance has a problem of noise caused by external vibration, a frequency filter using a digital PLL is added to the input circuit.

3. Cylindrical Resonator and Its Applications

3.1 Structure and Principles of the Resonator¹⁷⁾

Figure 8 shows the basic structure of a cylindrical resonator where n is the wave number of the circumferential flexural vibration, and m is the axial mode number. It consists of a thin-walled cylinder and a holder with sufficient rigidity and mass, and it has a similar cross-section, which includes the center axis of the cylinder, to that of the dual-ended tuning fork resonator. Therefore, as was mentioned in

section 2.1, vibration energy cannot easily escape outside, leading to a high mechanical Q (1×10^4 or more).

Applying pressure to the inner surface of the cylinder increases the internal tension of the cylinder, which increases its natural frequency. For a cylinder filled with a high-density fluid, its mass also increases as the natural frequency falls. Gas pressures or liquid densities can be calculated by taking advantage of such effects for measuring the natural frequency of a cylindrical resonator.

Vibration modes of the cylindrical resonator can be expressed by a combination of n and a wave number of the axial flexural vibration $m/2$. The natural frequency $f_{mn(0)}$ of the vibration mode of a cylinder in a vacuum can be calculated from equation (7) using the minimum real root Δ_{mn} of cubic equation (6):

$$\Delta_{mn}^3 + A_{mn}\Delta_{mn}^2 + B_{mn}\Delta_{mn} + C_{mn} = 0 \quad (6)$$

where

A_{mn} , B_{mn} , and C_{mn} : constants

determined by the structure, vibration mode number, boundary condition of cylinder, and Poisson's ratio ν of the material

$$f_{mn(0)} = \frac{1}{2\pi R} \left\{ \frac{E\Delta_{mn}}{\rho(1-\nu^2)} \right\}^{1/2} \quad (7)$$

where

- R : radius of the cylinder
- E : Young's modulus of cylinder material
- ρ : density of the cylinder.

The pressure sensitivity S_{mn} , the rate of frequency change per unit pressure for the vibration mode $\langle m, n \rangle$ when an internal pressure P is applied to a cylinder as shown in figure 8, can be expressed by equation (8)^{17, 18}:

$$S_{mn} = \frac{1}{2} \frac{(1-n^2)^2}{1+n^2} \cdot \frac{R}{h} \cdot \frac{1-\nu^2}{E\Delta_{mn}} \quad (8)$$

where

- h : thickness of the cylinder wall.

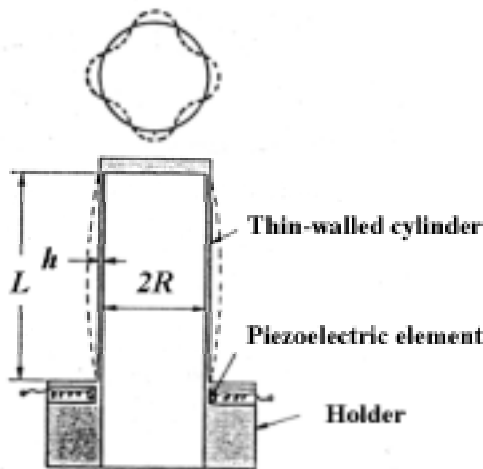


Figure 8. Structure of Cylindrical Resonator and Typical Vibration Mode ($m = 1, n = 4$)

Meanwhile, an apparent mass increment M per unit area when the cylinder is filled with a fluid with a density of ρ_x is approximately given by equation (9)¹⁹:

$$M \cong \rho_x \cdot R/n. \quad (9)$$

Consequently, the density sensitivity D_{mn} , the rate of frequency change per unit density for the vibration mode $\langle m, n \rangle$, can be expressed by equation (10):¹⁹

$$D_{mn} = -\frac{1}{2} \frac{1}{\rho_x \left(\frac{\rho}{\rho_x} \cdot \frac{h}{R} \cdot n + 1 \right)}. \quad (10)$$

Then the natural frequency f_{mn} of the cylinder can be given by the following equation (11), which can be derived from equations (8) to (10):

$$f_{mn}^2 \cong f_{mn(0)}^2 (1 + 2D_{mn}\rho_x)(1 + 2S_{mn}P). \quad (11)$$

3.2 Application to Barometer

We have applied the cylindrical resonator to the development of a precision barometer with extremely little aging. The cylindrical resonator is made of a nickel alloy with an excellent modulus of elasticity. However, even such an excellent material generates a slight temperature error or drift, which together with contamination or rust on the vibrating surface causes a change in natural frequency. Therefore, for accurate measurement of absolute pressure, barometric pressure in particular, we devised a method of exciting the pressure transducer in two vibrational modes at the same time that can theoretically eliminate these influences, and produced desired results.

When equation (7) is modified to allow for such disturbances as the linear expansion coefficient of material, the temperature coefficient of elastic material, and aging or contamination or rust on the vibrating surface, the natural frequency $f_{mn(0)}$ of the cylinder can also be empirically given by equation (12):

$$f_{mn(0)} = \frac{1}{2\pi R} \left\{ \frac{E\Delta_{mn}}{\rho(1-\nu^2)} \right\}^{1/2} (1 + \alpha T) \times \left(1 + \beta \log \frac{t}{t_0} \right) \quad (12)$$

where

ρ' : equivalent density of vibrating surface allowing for contamination

- α : temperature coefficient of material
- T : deviation from standard temperature
- β : effect of drift with time
- t : elapsed time
- t_0 : initial time.

Now using equation (12), the ratio r of the natural frequency in the vibration mode $\langle i, j \rangle$ to that of the mode $\langle k, l \rangle$ is as per equation (13):

$$r = \left(\frac{\Delta_{ij}}{\Delta_{kl}} \right)^{1/2}. \quad (13)$$

This means that r is not affected by temperature, elapsed time, or contamination of the vibrating surface. In addition, the rate of change in r for pressure P can be obtained from equation (14) using equation (11):

$$\frac{1}{r} \frac{dr}{dP} = S_{ij} - S_{kl} \quad (14)$$

Figure 9 shows the relationship between vibration mode numbers and pressure sensitivity of the barometric pressure transducer. We chose the vibration mode <1, 2>, which has the smallest pressure sensitivity, and <1, 4> with a large pressure sensitivity to improve various characteristics.

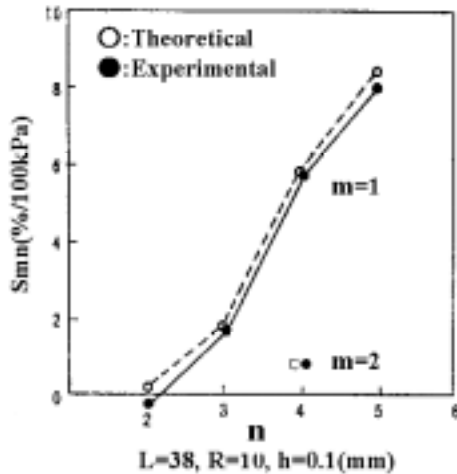


Figure 9. Relationship between Vibration Mode Number and Pressure Sensitivity

Figure 10 shows the configuration of the dual-mode oscillator circuit. The self-exciting cylindrical resonator oscillates in two modes of <1, 2> and <1, 4> independently and asynchronously. The terminals of the piezoelectric elements attached to vibrating nodes of the cylinder are represented by *a*, *b*, *c*, and *d*, where *a* and *b* are strain detection, while *c* and *d* excitation. The voltages generated in terminals *a* and *b* are in the same phase for the vibration mode <1, 4>, but are in reverse phase for the mode <1, 2>. They are therefore subtracted at point *e* and summed at point *f* to extract the voltage signals representing the two modes. Then the extracted voltage signals are controlled by a low-pass filter (LPF) and an automatic gain controller (AGC) in order for their phases and gains to meet oscillating conditions, and return back to terminals *c* and *d* for excitation.

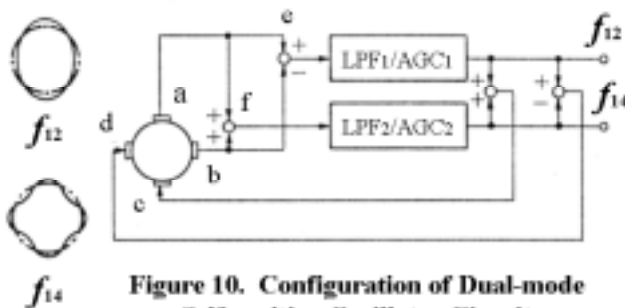


Figure 10. Configuration of Dual-mode Self-exciting Oscillator Circuit

Figure 11 shows the structure of the barometric pressure transducer. Atmospheric pressure is applied to the inner surface of the cylinder, and the outer surface is held at a reference vacuum level of 10^{-5} torr {1/760 Pa} or more with the casing. As barometric pressure is

nonlinear to the frequency ratio, a microcomputer calculates the pressure using a cubic equation as in the case of the pressure transducer using the dual-ended tuning fork resonator. After the pressure calibration, a repeatability better than ± 0.1 mbar was obtained within the range of 0 to 1000 mbar.

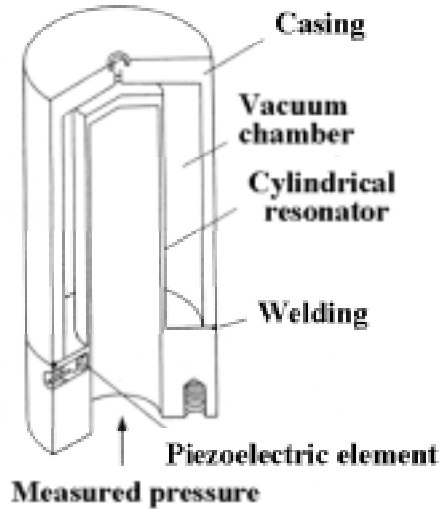


Figure 11. Structure of Barometric Pressure Transducer

Figure 12 shows measurement data when attaching magnesium oxide to the surface of the cylinder for testing the effect of dual-mode oscillation. It is clear that the dual-mode oscillation, which outputs the natural frequency ratio, has improved the effect of contamination by an order of magnitude compared to the single-mode oscillation. The same goes for aging and a one-year performance test confirmed that the pressure drift was accurate within ± 0.1 mbar based on a standard mercury barometer.

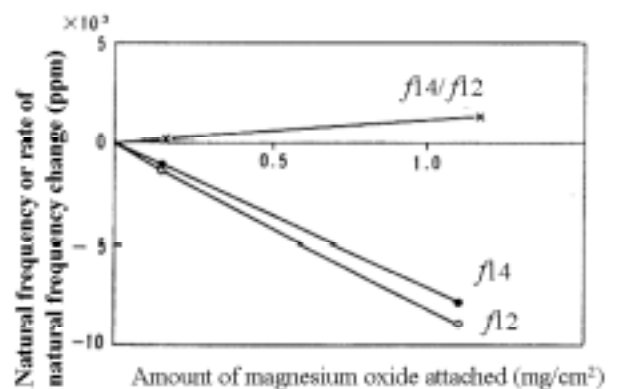


Figure 12. Effects of Dual-Mode Oscillation Method

3.3 Application to Differential Pressure Transducer^{20), 21)}

Since the cylindrical resonator has such parameters as the pressure sensitivity and density sensitivity shown in equation (11), it is necessary to consider the effect of static pressure (density) for measuring differential pressure ($P_1 - P_2$). It is evident

from equation (10) that the density sensitivity is always constant for the same circumferential mode number n even if the axial mode number m varies. However, figure 9 indicates that the pressure sensitivity for $m = 1$ differs from that for $m = 2$, even if $n = 4$ for both of them. The ratio r_d between f_{14} and f_{24} can be calculated using equation (11):

$$r_d = \frac{f_{14}}{f_{24}} = \frac{f_{14(0)}}{f_{24(0)}} \left\{ \frac{1 + 2S_{14}(P_1 - P_2)}{1 + 2S_{24}(P_1 - P_2)} \right\}^{1/2} \tag{15}$$

$$\cong \frac{f_{14(0)}}{f_{24(0)}} (S_{14} - S_{24})(P_1 - P_2)$$

Therefore, choosing r_d as an output can eliminate the effects of static pressure, temperature, contamination on the vibrating surface, and aging, allowing for the implementation of a differential pressure transducer using a differential pressure sensitivity between two vibration modes.

Figure 13 shows the structure of a differential pressure transducer using this method. A differential pressure ($P_1 - P_2$) is applied to a cylindrical resonator. The terminals of the piezoelectric elements attached to vibrating nodes of the cylinder are represented by a , b , and c . The self-exciting cylindrical resonator oscillates in the same manner as for the barometer. In other words, the voltages generated in terminals a and b are in the same phase for the vibration mode $\langle 1, 4 \rangle$, but are in

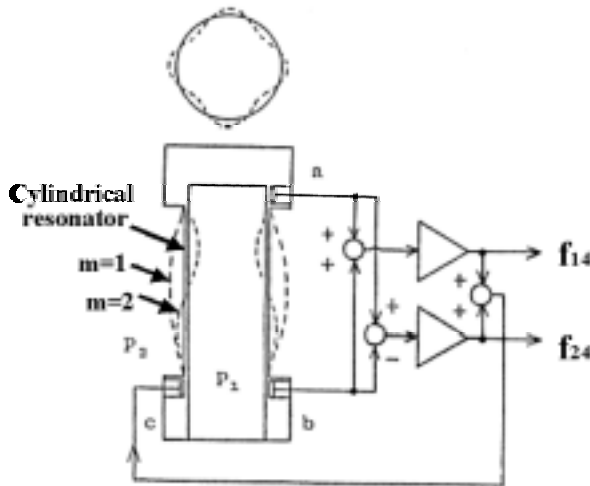


Figure 13. Structure of Differential Pressure Transducer

reverse phase for the mode $\langle 2, 4 \rangle$. They are therefore summed and subtracted to extract the two frequency signals.

Figure 14 shows the static pressure characteristics of the differential pressure transducer with a measuring range of 0 to 200 kPa, contrasted with a single mode pressure transducer. The residual errors probably resulted from the approximation by equation (9). But they can further be improved by compensating after one-point calibration for the static pressure.

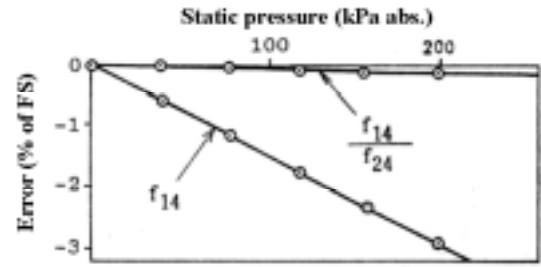


Figure 14. Static Pressure Characteristics of Differential Pressure Transducer

3.4 Application to Highly Environmental Resistant Absolute Pressure Transducer

We have developed a small, lightweight absolute pressure transducer that can be used in harsh environments susceptible to extreme vibration or temperature such as that of electronic control for aircraft engines. The cylindrical resonator transducer is unaffected directly by attitude or acceleration and thus is suitable for use in aircraft. Moreover, it has already achieved satisfactory results in testing in which it was mounted to an actual fan jet engine on the ground.

Figure 15 shows the structure and configuration of the absolute pressure transducer. Although it may look similar to that of the barometric pressure transducer, since it needs multi-measuring ranges, it does not adopt dual-mode oscillation so as to provide more design flexibility, with an eye on downsizing and weight reduction. Both ends of the resonator are welded to shift the natural frequency of the cylinder in the flexural mode to a higher bandwidth than the signal frequency for better vibration resistance.

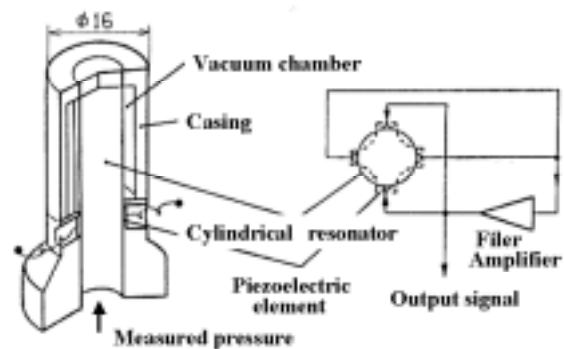


Figure 15. Structure and Configuration of Absolute Pressure Transducer

Figure 16 shows the calibration characteristics of the absolute pressure transducer at a measuring range of 0 to 700 kPa abs, and figure 17 the vibration resistance characteristics. The absolute pressure transducer has high accuracy and compensating temperature with the internal transducer can further improve the accuracy to $\pm 0.1\%$ of full scale when within -55°C to $+110^\circ\text{C}$.

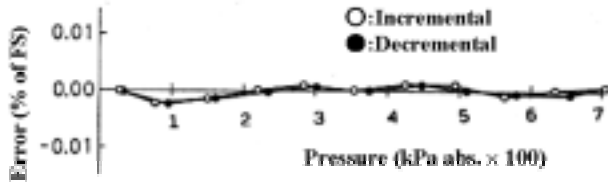


Figure 16. Calibration Characteristics of Absolute Pressure Transducer

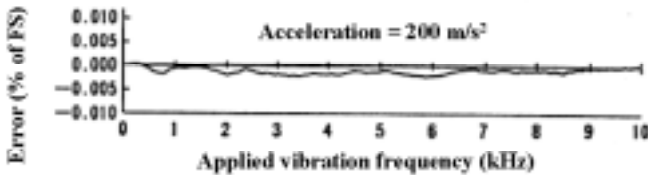


Figure 17. Vibration Resistance Characteristics of Absolute Pressure Transducer

3.5 Application to Portable Densimeter

Figure 18 shows the structure of a pencil-sized densimeter using a cylindrical resonator. Liquid density can be measured easily by dipping the probe tip into the sample liquid in a test tube when the cylinder is filled with liquid. As the natural frequency of the resonator varies depending on liquid density as shown in equation (10), the liquid density can be determined by measuring the natural frequency.

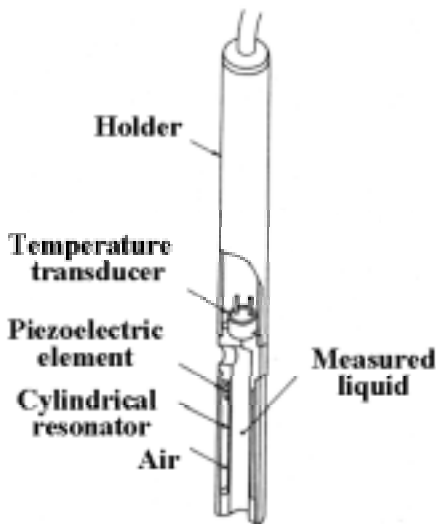


Figure 18. Structure of Portable Densimeter

Figure 19 shows the relationship between vibration mode numbers and density sensitivity. The densimeter uses the mode <1, 2>, which has a maximum density sensitivity and minimum pressure sensitivity. As the density is nonlinear to the cycle of resonant frequency, a microcomputer is used to compensate and linearize it.

If the liquid viscosity increases, resonant frequency f slightly decreases. This is because the increased density causes the liquid density to appear higher than it actually is. The following relationship (16) is maintained between the apparent density increment $\Delta\rho_x$ and the increment in damping ratio for vibration ΔC for Newtonian fluid:

$$\Delta C \propto f^2 \cdot \Delta\rho_x \quad (16)$$

If the exciting force is kept constant, ΔC can be obtained from the ratio of vibration amplitude changes. Therefore the densimeter eliminates the effect of viscosity by compensating for the apparent density increment produced by the change in viscosity which can be calculated from equation (16).

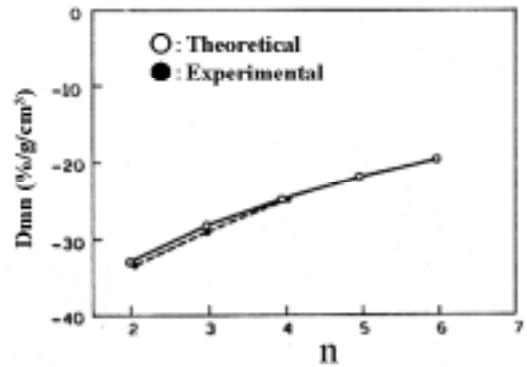


Figure 19. Relationship between Vibration Mode Number and Density in the Vicinity of $\rho_x = 1 \text{ g/cm}^3$

This densimeter has a small, lightweight sensor block, allowing density measurement of a sample liquid in several milliliter quantities with high accuracy. After calibration using the hydrostatic method, the error is less than $\pm 5 \times 10^{-4} \text{ g/cm}^3$ for liquids whose density is

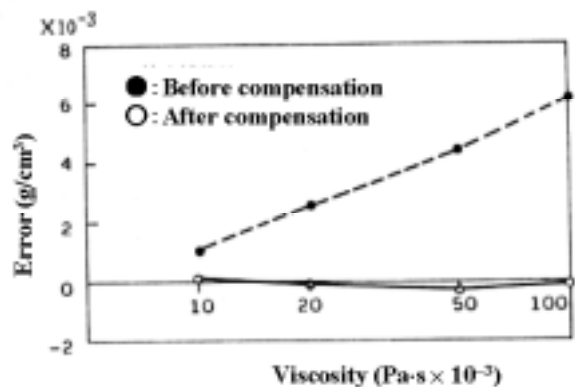


Figure 20. Viscosity Compensation Characteristics of Densimeter

0.6 to 1.5 g/cm^3 . Figure 20 shows the viscosity characteristics before and after compensation for comparison. The accuracy is $\pm 5 \times 10^{-4} \text{ g/cm}^3$ for liquids whose viscosity is up to 0.1 Pa·s, which demonstrates the excellent compensation capabilities.

4. Conclusion

Some of the resonator transducers described in this paper have already been commercialized. For example, an electronic balance using a resonator was released recently,²⁶⁾ and a barometer introduced on the market several years ago was favorably received.²⁷⁾ As for a highly environmental resistant absolute pressure transducer, various tests are being conducted in preparation for commercialization, and a densimeter will also be available very soon.

These transducers using mechanical resonators boast the following features compared with conventional transducers:

- 1) The frequency output signal can be easily converted into a digital signal with high resolution (e.g. 24 bits) at low costs.
- 2) The frequency output signal is compatible with a microcomputer, thus allowing simultaneous detection of multidimensional information to realize an intelligent transducer.
- 3) The transducer gives a wide frequency change for a small input. For a pressure transducer, the rate of frequency changes per unit strain ($\Delta f/f_0 \cdot 1/\Delta \varepsilon$) is approximately 500 to 1300. This means that the transducer can be designed with minimum strain applied to the resonator.
- 4) The transducer has high mechanical Q and thereby can give superior accuracy and repeatability using a simple electronic circuit.
- 5) The structured transducer allows uniform characteristics through proper management of design and machining accuracy.

We will pursue other transducers exploiting these features that are smaller and can be used in a wider range of applications.

The authors would like to take this opportunity to thank the late Dr. Isamu Ohno, Department Manager, Corporate R&D Department of Yokogawa Hokushin Electric Corporation for his advice and guidance during this work, and Mr. Motoyoshi Ando, Seiki Luo, Daisuke Yamazaki, Kouichi Arashida, and others for their contribution to the experiments.

References

- 1) G. Arvidson: Device for Pressure or Difference of Pressure in Fluid, US Pat. 3021711 (1962)
- 2) A. M. Voutsas: Twisted Beam Transducer, AIAA Journal, 1-4, 911/913 (1963)
- 3) R. J. Halford: Pressure Measurement Using Vibrating Cylinder Pressure Transducer, Instrument Practice, 18-8, 823-829 (1964)
- 5) P. N. Potter: Frequency Domain Transducers and their Applications, Instrument Practice, 23-12, 849/853 (1969)
- 6) J. M. Paros: Precision Digital Pressure Transducer, ISA Trans., 12-2, 173/179 (1973)

- 7) P. R. Wyman: A New Force to Frequency Transducer, IEE Conf. Publication, 106, 117/123 (1973)
- 8) G. M. Shuster: On the Use of Resonant Diaphragms as FM Pressure Transducers, IEEE Trans., IECI 25-1, 29/38 (1978)
- 9) C. W. Doran: A New Standard for Electronic D/P Transmitter Selection, ISA Annual Conf., 457/462 (1978)
- 10) K. Harada, K. Ikeda, T. Ueda: Development of Precision Transducers Using Mechanical Resonators, Yokogawa Technical Report, 26-2, 55-61, (1982), in Japanese
- 11) T. Ueda, F. Kohsaka: Force Transducers Using Mechanical Resonator, Proc. of 19th Conf. of SICE, 541-542, (1982), in Japanese
- 12) T. Ueda, F. Kohsaka, E. Ogita: Precision Force Transducers Using Mechanical Resonators, Proc. of 10th Conf. of IMECO TC-3 on Meas. Force and Mass, 17/22 (1984)
- 13) Okumura, Inukai: Approximate Equations for Resonant Frequency of beam Resonator with Axial Force, JSME, 17-57, 8/13(1951), in Japanese
- 14) T. Ueda, F. Kohsaka: Pressure Transducer Using Mechanical Resonator, Proc. of 20th Conf. of SICE, 659-660(1981), in Japanese
- 15) T. Ueda, F. Kohsaka, D. Yamazaki: Compact and Precision Pressure Transducer Using Mechanical Resonator, Proc. of 23th Conf. of SICE, 113-114(1984), in Japanese
- 16) T. Ueda, S. Luo, Nakamura: Electronic Balance Using Mechanical Resonator, Proc. of 20th Conf. of SICE, 665-666(1981), in Japanese
- 17) K. Ikeda: Pressure Transducer Using Cylindrical Resonator with Dual-mode Self-exciting Oscillation Technique, SICE, 18-7, 710/715(1981), in Japanese
- 18) R.N. Arnold and G.B. Warburton: The Flexural Vibration of Thin Cylinders, Proc. of Institution of Mechanical Engineers, 167, 62/80 (1953)
- 19) M.K. Au-Yang: Free Vibration of Fluid-coupled Coaxial Cylindrical Shells of Different Length, Trans. Of ASME, Journal of Applied Mechanics, 480/484 (1976)
- 20) K. Ikeda, K. Isozaki: Differential Pressure Transducer Using Cylindrical Resonator, Proc. of 23rd Conf. of SICE, 115-116(1984), in Japanese
- 21) K. Ikeda, K. Isozaki: Multidimensional Information Transducer Using Resonant sensor, Proc. of 23rd Conf. of SICE, 677-678(1984), in Japanese
- 22) K. Ikeda, K. Arashida: High Environmental Resistant Absolute Pressure Transducer Using Cylindrical Resonator, Proc. of 22nd Conf. of SICE, 261-262(1983), in Japanese
- 23) Arahata, Tsumura, Arashida: Ikeda, Pressure Transducer for Electronic Control for Aircraft Engines, Proc. of 20th Conf. of SICE, 401-402(1981), in Japanese
- 24) Ikeda, Ando, Isozaki: Development of Portable Densimeter Using Cylindrical Resonator, Proc. of 20th Conf. of SICE, 401-402(1981), in Japanese
- 25) K. Ikeda and K. Isozaki: A Precision Densimeters which Compensates for Liquid Viscosity, IEEE Trans., Vol. IM-35, No.4, Dec. (1986)
- 26) Nishiguchi: Electronic Balance Using Double-ended Tuning Fork Resonator, Proc. of 3rd Meeting of

Mass and Force Measurement SICE, 27-30(1983), in Japanese
27) F451 Barometer using Cylindrical Resonator, Catalog of Yokogawa Densikiki Co., Ltd, in Japanese



Kinji Harada (Member)



He received the B.S. degree in precision engineering from Osaka University in 1960. He joined Yokogawa Electric Corporation in 1960 and was mainly engaged in the R & D of sensors and sensing technologies. Since 1997, he has been with Yokogawa Research Institute Corporation where he has been working for the regional consortium projects to develop micromachining instruments.

Kyoichi Ikeda (Member)



He was born in 1940 in Nagaoka, Japan. In 1963 he received B.S. degree in Precision Machinery Engineering from Niigata University. In 1990, he received Ph.D. degree from University of Tokyo. From 1963 to 1999 he joined Yokogawa Electric Corporation and was working on research and development of

Sensors and Micro Electro Mechanical Systems. He was awarded Grand Okohchi Memorial Prize in 1994 for research on silicon resonant pressure sensors. From 1999 he has been a professor of the Department of Mechanical Systems Engineering in Tokyo University of Agriculture and technology. He is a member of IEEE and an editorial board member of Journal of Micromechanics and Microengineering in Institute of Physics.

Toshitsugu Ueda (Member)



Toshitsugu Ueda was born in Nara, Japan, on October 4, 1945.

He received the B.E. and M.E. degree in electrical engineering from Shinshu University, Nagano, Japan, in 1969 and 1971 respectively.

He received Ph.D. degree from Tokyo Institute of Technology in 1988. Since joining Yokogawa Electric Corporation in 1971, he has been engaged in developing low noise amplifiers, mechanical resonators, micro machining technologies and sensors using above mentioned technologies for temperature, pressure and displacement. Now he is a general manager of Corporate R&D department.

He received Awards from Society of Instrument and Control Engineers of Japan in 1987 and 1994, and

Awards from Japan Institute Invention and Innovation in 1985 and 1987. Dr. Ueda is a member of the Institute of Electrical Engineers of Japan, and Society of Instrument and Control Engineers of Japan.

Fusao Kousaka (Member)



He received the B.E. degree in Mechanical Engineering from Akita University. Since 1975, he researched the Sensors and Micro Mechanical Devices. From 1997, he is developing the Liquid Crystal Display System for Aerospace applications.

Katsumi Isozaki (Member)



He was born in 1957. He received the B.S. degree in Electrical Engineering from Tokyo Denki University in 1980. He joined Yokogawa Electric Corporation in 1980. Since then, he has been engaged in research and development of sensors and sensing technologies. He

developed Portable Densimeter, Precision Range Finder System, Confocal Microscopy (CSU-10) and FT-NIR Analyzer (NR800).



Reprinted from Trans. Of the SICE, Vol.24, No.8, 75/82 (1987)